



King Saud University

Arabian Journal of Chemistry

www.ksu.edu.sa  
www.sciencedirect.com



## ORIGINAL ARTICLE

# Potential bioactive secondary metabolites of Actinomycetes sp. isolated from rocky soils of the heritage village Rijal Alma, Saudi Arabia



Saad S. Alqahtani<sup>a,b</sup>, Sivakumar S. Moni<sup>c,\*</sup>, Muhammad H. Sultan<sup>c</sup>, Mohammed Ali Bakkari<sup>c</sup>, Osama A. Madkhali<sup>c</sup>, Saeed Alshahrani<sup>d</sup>, Hafiz A. Makeen<sup>a,b</sup>, Santhosh Joseph Menachery<sup>a,b</sup>, Zia ur Rehman<sup>e</sup>, Md Shamsheer Alam<sup>e</sup>, Syam Mohan<sup>f,g</sup>, Mohamed Eltaib Elmobark<sup>c</sup>, David Banji<sup>d</sup>, Mohamed Z. Sayed-Ahmed<sup>a,b</sup>

<sup>a</sup> Clinical Pharmacy Department, College of Pharmacy, Jazan University, Jazan, Saudi Arabia

<sup>b</sup> Pharmacy Practice Research Unit, College of Pharmacy, Jazan University, Jazan, Saudi Arabia

<sup>c</sup> Department of Pharmaceutics, College of Pharmacy, Jazan University, Jazan, Saudi Arabia

<sup>d</sup> Department of Pharmacology and Toxicology, College of Pharmacy, Jazan University, Jazan, Saudi Arabia

<sup>e</sup> Department of Pharmaceutical Chemistry, College of Pharmacy, Jazan University, Jazan, Saudi Arabia

<sup>f</sup> Substance Abuse and Toxicology Research Centre, Jazan University, Jazan, Saudi Arabia

<sup>g</sup> School of Health Sciences, University of Petroleum and Energy Studies, Dehradun, Uttarakhand, India

Received 15 December 2021; accepted 10 February 2022

Available online 14 February 2022

## KEYWORDS

Actinomycetes species;  
Lab-scale fermentation;  
Secondary metabolites;  
Antibacterial effect

**Abstract** The present study was designed to discover novel secondary antibiotic metabolites from Actinomycetes species from the soil of Rijal Alma, Saudi Arabia. A laboratory-scale benchtop fermentation was utilized for the demonstration of antibiotics from the soil actinomycetes. Fourier transform-infrared spectroscopy (FT-IR) spectroscopy analysis of the fermented product (FP) was carried out, which showed unique fingerprint regions indicating the presence of phenolic hydroxyl groups, aliphatic compounds, carboxylic groups, esters, isothiocyanate, etc. GC-MS analysis of the FP depicted the unique structures of secondary metabolites, such as cyclononasiloxane octadecamethyl, cercosporin, ethyl *iso*-allochololate, octadecane, 3-ethyl-5-(2-ethylbutyl), dasycarpidan-1-methanol (acetate), heptadecane, 9-hexyl-, phthalic acid-butyl, and octadecane, 3-ethyl-5-(2-ethylbutyl). The TGA analysis showed the thermal stability of FP and the initial weight loss in FP was observed at 277.29 °C. The <sup>1</sup>H NMR and <sup>13</sup>C NMR spectra of FP analysis demonstrated the various characteristic peaks presence of secondary metabolites. The XRD analysis at 2θ revealed distinct particles based on specific diffraction peaks. A set of six human bacterial pathogens, namely, the Gram-positive bacteria *Staphylococcus aureus* (*S. aureus*), *Streptococcus pyogenes* (*S. pyogenes*), and *Bacillus subtilis* (*B. subtilis*) and Gram-negative bacteria *Escherichia coli* (*E. coli*), *Pseudomonas aeruginosa* (*P. aeruginosa*), and *Klebsiella pneumoniae* (*K. pneumoniae*), were utilized

\* Corresponding author.

E-mail addresses: drsmsivakumar@gmail.com, smoni@jazanu.edu.sa (S.S. Moni).

for screening. The FP exhibited promising antibacterial effects against both Gram-positive and Gram-negative bacterial organisms. The antibacterial spectrum of activity was greater for *E. coli* and *B. subtilis* than for *K. pneumoniae*.

© 2022 The Author(s). Published by Elsevier B.V. on behalf of King Saud University. This is an open access article under the CC BY license (<http://creativecommons.org/licenses/by/4.0/>).

## 1. Introduction

The complications of antibiotic resistance have spiked sharply in recent years and have become a substantial threat to humans worldwide, critically causing enormous morbidity and mortality in humans (Catalano et al., 2022; Chloe, 2022). According to studies conducted in Saudi Arabia, the problems of microbial resistance are increasing significantly in terms of the prevalence of extended-spectrum beta-lactamase (ESBL) among *Escherichia coli* (*E. coli*) and 65% ESBL rates among *Klebsiella pneumoniae* (*K. pneumoniae*). Saudi national surveillance on Gram-positive cocci reported that 32% of *Staphylococcus aureus* (*S. aureus*) are methicillin-resistant *S. aureus* (MRSA) and that 33% and 26% of *Streptococcus pneumoniae* are resistant to penicillin G and erythromycin, respectively (Zowawi, 2016). The Global Antibiotic Research and Development Partnership (GARDP), a joint initiative of the World Health Organization (WHO) and Drugs for Neglected Diseases initiative (DNDi), is encouraging research and development through public-private partnerships to develop new treatments by discovering newer wide-spectrum antibiotics. Therefore, the scientific communities have become highly competitive and seriously engaged in developing new antibiotic molecules to cure various ailments. Almost all commercially available antibiotics have become ineffective, posing a significant threat to the current therapeutic world. In addition, the entire world population is currently ravaged with known and unknown origins of pathogens. This situation has necessitated and compelled scientists to develop novel antibiotics (Miethke et al., 2021; Moni et al., 2018; Safhi et al., 2016).

The discovery of new antibiotics and antibacterial agents, therefore, is essential in modern medicine. Actinomycetes are the most abundant higher bacteria that form fungi-like hyphae, and they are highly ubiquitous and widely distributed in the soil. The diversity of Actinomycetes is of extraordinary significance in antibiotic production (Selim et al., 2021; Mukesh et al., 2014; Magarvey et al., 2004; Lazzarini et al., 2000). These bacteria are industrially beneficial microorganisms that produce a wide variety of antibiotics and are involved in producing antibiotics of significant interest to the pharmaceutical industry.

The purpose of this work was to develop a novel antibiotic from natural sources that can overcome the drug resistance associated with conventional antibiotics, especially multiple drug resistance, which is a threat to day-to-day therapeutic implementation (Catalano et al., 2022; Hawkey et al. 2018; Barsby et al., 2001). Bacterial resistance occurs through various mechanisms such as efflux pumps and exocytosis as well as due to drug misuse and irrational drug therapy (Byrne et al., 2019). To overcome this situation, there are two approaches, either rationalizing the therapy or discovering novel antibiotics with a broad spectrum of activity (Taswar

et al., 2017; Parungao et al., 2007). The governments of most of the countries in the world are implementing many restrictions to minimize or stop the misuse of antibiotics (Rogers Van Katwyk et al., 2019). Therefore, we opted to discover newer biochemical entities from soil actinomycetes to end the pathogen threat. Consequently, our study has also emphasized the identification of secondary metabolites/novel antibiotic molecules from actinomycete species isolated from the soil of Rijal Alma, Saudi Arabia.

## 2. Material and methods

### 2.1. Isolation of actinomycetes

The study area was Rijal Alma, which is located 45 km towards west from the city Abha that coordinates N 2015840.65 and E 211634.87. Rijal Alma is located in Asir province in the Southern region of Saudi Arabia. The village Rijal Alma is a natural corridor that links Yemen and Saudi Arabia. Rijal Alma is a mountainous area bordered to the east by Al-Souda Center, from the north by Muhayil Asir province and from the south by Al-Darb province. The soil sample was collected from the riverbed of Rijal Alma in an aseptic polyethylene bag. The sampling was done from 10 to 12 cm of soil using an axe (Fig. 1). After collection, the soil sample was transferred to the laboratory for processing. The soil was sieved through a no. 10 sieve, weighed, and pooled. The pooled soil was kept in a hot air oven at 60 °C for 1 h to remove moisture. Then, 10 g of sterilized soil sample was added to a 250 mL container with 100 mL of distilled sterile water and stirred at 3000 rpm for 30 min using a magnetic stirrer. A few drops of tween 80 were added to reduce the foam formation during stirring. The soil solution was serially diluted in Millipore water using a two-fold serial dilution method down to 10<sup>-6</sup>. Sabouraud dextrose (SD) agar plates were prepared, 100 μL of soil solution was placed on the SD agar plates, and the solution was spread thoroughly on the agar surface using the spread plate technique. The inoculated plates were incubated at 37 °C for 72 h and were observed for colony formation. Actinomycetes were identified by a simple Gram staining technique for the identification of bacteria and lactophenol blue staining for the fungal mycelial structure. The mycelial structure was also confirmed using the agar block technique. In this process, SD agar plates were prepared, and a 1 × 1 cm block was cut down with a sterile blade. The isolated organism was streaked on the agar block. Then, the block was incubated at 32 °C for 72 h and evaluated for colonies with mycelial (hyphal) structures. The hyphal structure was observed using a lactophenol blue stain under a phase-contrast microscope at 10 and 20×, Nikon NS 100 Phase contrast microscope, Japan. The characteristic features were observed and noted for further studies. Biochemical tests such as starch hydrolysis, methyl red test, indole test, Vogus-Proskauer, triple sugar iron test, and

catalase test were performed as reported earlier (Mary Ann and John, 1967; Chaudhary et al., 2013a).

## 2.2. Fermentation protocol

Laboratory-scale fermentation was performed using predetermined media for approximately 5 days at room temperature with constant shaking. The isolated strain was sub-cultured in 25 mL of SD broth and incubated at 32 °C for 72 h. After incubation, the broth containing the actinomycetes growth was designated as seed culture. The working formula of the fermentation medium was 70% tryptone soya broth, 20% Sabouraud dextrose broth, 10% peptone water, and 200 mL

of Millipore water. The pH was observed to be 7–7.5, and the type of fermentation was aerobic. All the media were mixed in 200 mL of Millipore water and then transferred into a 500 mL glass conical flask. The conical flask was pugged tightly with sterile non-absorbent cotton and tightly covered with aluminium foil. The medium was sterilized in an autoclave at 15 psi and 121 °C for 20 min, transferred to a laminar air hood and allowed to cool to room temperature. Thereafter, 5 mL of seed culture was transferred to 200 mL of fermented media. Then, the flask was kept in a flask shaker at 176 rpm at room temperature for 5 days. Purification of fermented liquid was performed to remove the unwanted cellular debris and mycelial content. The fermented liquid was subjected to col-

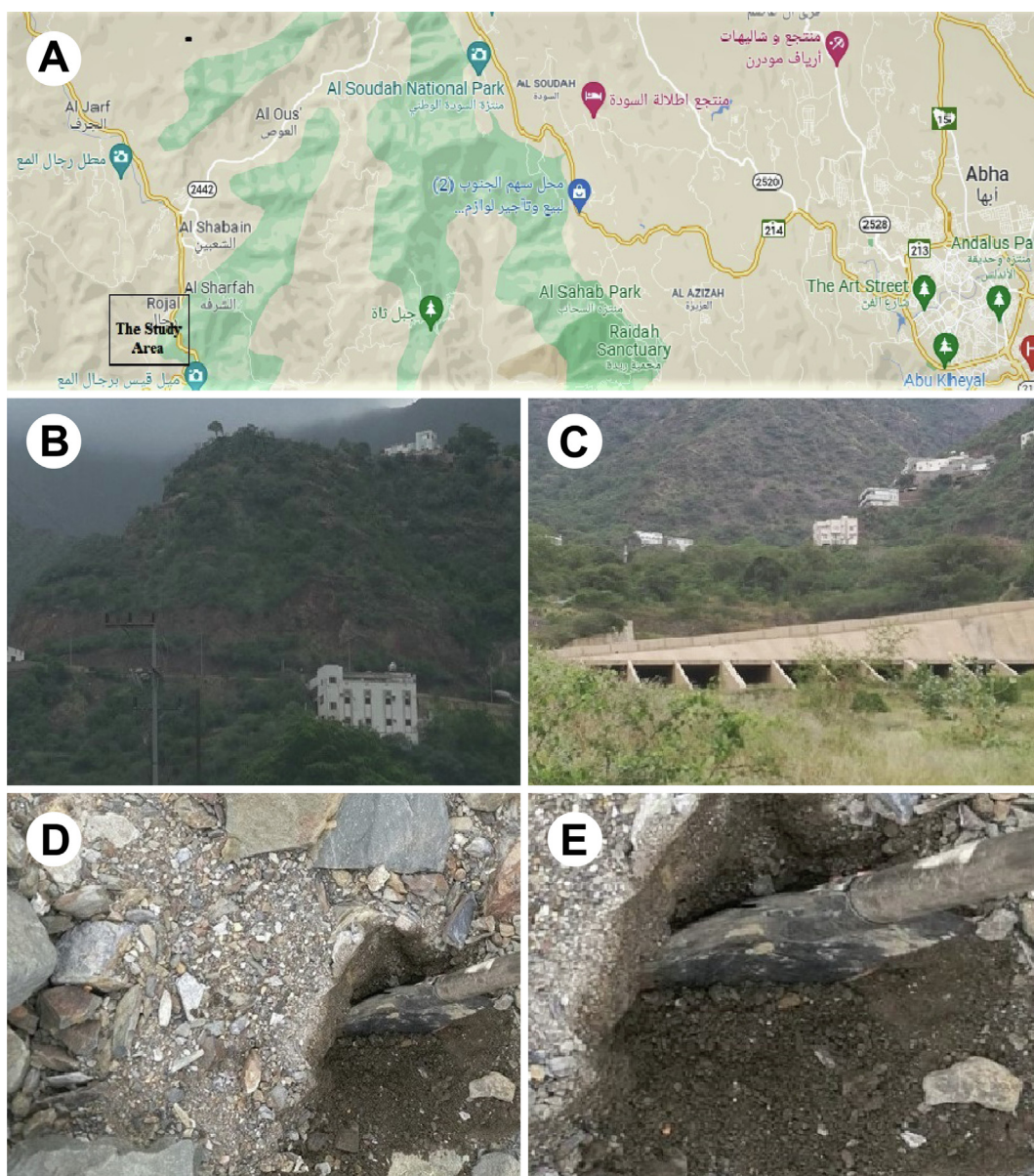


**Fig. 1** The Study area. (A) Rijal Alma region is located 45 km west of the city of Abha, that coordinates N 2015840.65 and E 211634.87 which is a mountainous area bordered to the east by Al-Souda Center, and from the North Muhayil Asir province; (B & C) The view of hills in Rijal Alma from soil collection point; (D) The soil was collected by digging at 10 to 12 cm depth by using Axe cutter; (E) The Depth of soil collection point.

umn chromatography by using silica gel 60 (Sigma-Aldrich, USA), and fractions were collected; then, the fraction was centrifuged at 3000 rpm (Sigma, USA) for 15 min. Once the cellular debris settled, the supernatant was separated for further processing. To the supernatant, 95% v/v ethanol was added, and the same centrifugation process was carried out for 15 min. Ethanol treatment was performed to remove higher molecular weight toxic proteins such as cellular metabolites. The purified fermented fraction was passed through syringe filters containing a PVDF membrane (0.2  $\mu\text{m}$  pore size), which was designated the fermented product (FP). The FP was subjected to various analyses to characterize its properties.

### 2.3. Zeta potential, size, and PDI analyses

The zeta potential (ZP), particle size distribution, and polydispersity index (PDI) of the FP were evaluated by using a Nano-ZS Zetasizer (Malvern Instruments, UK). These analyses are used to physically characterize the colloidal liquid products to determine the surface charges of dispersed molecules, the Brownian movement of dispersed molecules, and the size of dispersed particles in the FP.

### 2.4. FT-IR spectroscopy

The specific functional groups in the FP were analysed by FT-IR spectroscopy using a Nicolet iS10 FT-IR spectrophotometer (Thermo Scientific, USA). A simple KBr pellet technique was performed, and spectra of the pellet sample were obtained via the FT-IR spectrophotometer against a reference KBr pellet in the range of 400–4000  $\text{cm}^{-1}$ , with a resolution of 4  $\text{cm}^{-1}$ .

### 2.5. GC-MS analyses

The presence of possible bioactive compounds in the FP was determined by gas chromatography-mass spectrometry (GC-MS, Thermo Scientific TR, USA). The GC-MS instrument was equipped with an AS 3000 autosampler, trace ultra-GC, and ISQ detector. The FP was diluted in methanol to a volume ratio of 1:10. The mass spectra were interpreted using Xcalibur software, and the fragmentation patterns of the mass spectra were compared with those stored in the spectrometer database using NIST, MAINLIB, and REPLIB built-in libraries.

### 2.6. Lyophilization process

The FP was lyophilized using a Millrock BT85 tabletop freeze dryer, Millrock Technology, USA, as previously reported (Madkhali et al., 2021). Mannitol solution (5% w/v) was combined with the FP reaction mixture at a volume ratio of 2:1 in a glass flask. The combination was kept at  $-80\text{ }^{\circ}\text{C}$  in a deep freezer for 24 h. Following that, the glass flask was placed in lyophilizing tubes, and the vacuum was induced by opening the knob. The temperature was maintained at  $-84\text{ }^{\circ}\text{C}$ , and the vacuum was kept at 3000 Pa (Pascals). After 30 h of lyophilization, the lyophilized nanoparticle powder was eluted from the glass flask, pooled, and kept at  $+4.0\text{ }^{\circ}\text{C}$  until used in the subsequent study.

### 2.7. Thermogravimetric analysis (TGA)

The thermal stability of the samples in an air atmosphere was assessed using a thermogravimetric analyser (TGA 8000, Perkin Elmer, USA). The lyophilized FP powder sample (10 mg) was placed on an aluminium pan, and the test was conducted at a heating rate of  $10\text{ }^{\circ}\text{C}/\text{min}$  within a temperature range of  $50\text{--}300\text{ }^{\circ}\text{C}$ .

### 2.8. Nuclear magnetic resonance (NMR) spectroscopy

The lyophilized FP was subjected to nuclear magnetic resonance (NMR) spectral analysis. Samples were previously prepared in deuterated water ( $\text{D}_2\text{O}$ ). The NMR spectrum of the crystal sample was recorded on Bruker 400 Ultra shield NMR spectrometer operating at 400 MHz to obtain  $^1\text{H}$  NMR, and at 100 MHz for  $^{13}\text{C}$  NMR.

### 2.9. X-Ray diffraction (XRD) analysis

The lyophilized FP powder samples were evaluated using X-ray diffraction (XRD). X-ray powder diffraction of the samples was evaluated by Ultima IV diffractometer (Rigaku, USA). The XRD diffractograms were obtained at  $2\theta$  in the range of  $3\text{--}140^{\circ}$  using Cu K  $\alpha$  radiation of incident Ultima IV diffractometer beam ( $\lambda = 1.5418\text{ \AA}$ ) at a voltage of 45 kV and a current of 0.8 mA. A scanning range of  $2\theta/\theta$  was selected and scanning speed of  $10\text{ min}^{-1}$  was employed. The tube anode was Cu with  $\text{K}\alpha = 0.1540562\text{ nm}$  monochromatized with a graphite crystal. The pattern was collected at 40 kV of tube voltage and 40 mA of tube current in step scan mode (step size  $0.02^{\circ}$ , counting time 1 s per step).

### 2.10. Assessment of antibacterial activity

The bacterial strains *S. aureus*, *S. pyogenes*, *B. subtilis*, *E. coli*, *P. aeruginosa*, and *K. pneumoniae* were used in the investigation. 24 h cultures were prepared and standardized using nutrient broth gradient dilutions ranging from  $10^{-1}$  to  $10^{-7}$ . The vitality of bacterial cultures was assessed by counting the colony-forming units (CFU) per millilitre (mL). The antimicrobial susceptibility test was performed using the method developed by Moni et al. 2018. To conduct the antibacterial study, Mueller Hinton agar plates were constructed. Bacterial cultures were subcultured from the stock culture and then exposed to antibacterial examination after 24 h of incubation. The organisms were grown using the spread plate technique. The FP sample (Test sample) was diffused using the agar well technique, whereas the standard (Control) ciprofloxacin disc (5 mcg/disc) was diffused using the disc diffusion technique. Individual cultures were inoculated by dipping a sterile cotton swab into standardized (CFU/mL) concentrations and streaking over MH agar plates while rotating the petri dish to ensure uniform distribution of the culture. The inoculation method was done twice for optimal culture growth. Before administering FP sample, the plates were allowed to dry for approximately 10 min. Following that, wells were made on MH agar plates by punching holes with a stainless-steel borer. The wells were 10 mm in diameter, and the FP sample was administered

in the appropriate wells. The disc diffusion technique was conducted by gently pressing the ciprofloxacin disc into the agar surface with sterilized forceps. After 24 h of incubation at 37 °C, the antibacterial spectrum was determined by the formation of inhibitory zones. The activity spectrum is directly proportional to the diameter of the inhibition zones. The zone's diameter was determined and documented.

### 3. Results and discussion

The screening of secondary microbial products from actinomycetes species has contributed significantly to the discovery of novel antibiotics for combating various infectious diseases (Taswar et al., 2017; Gupta and Gupta, 2017). The present study focused on the development of secondary metabolites

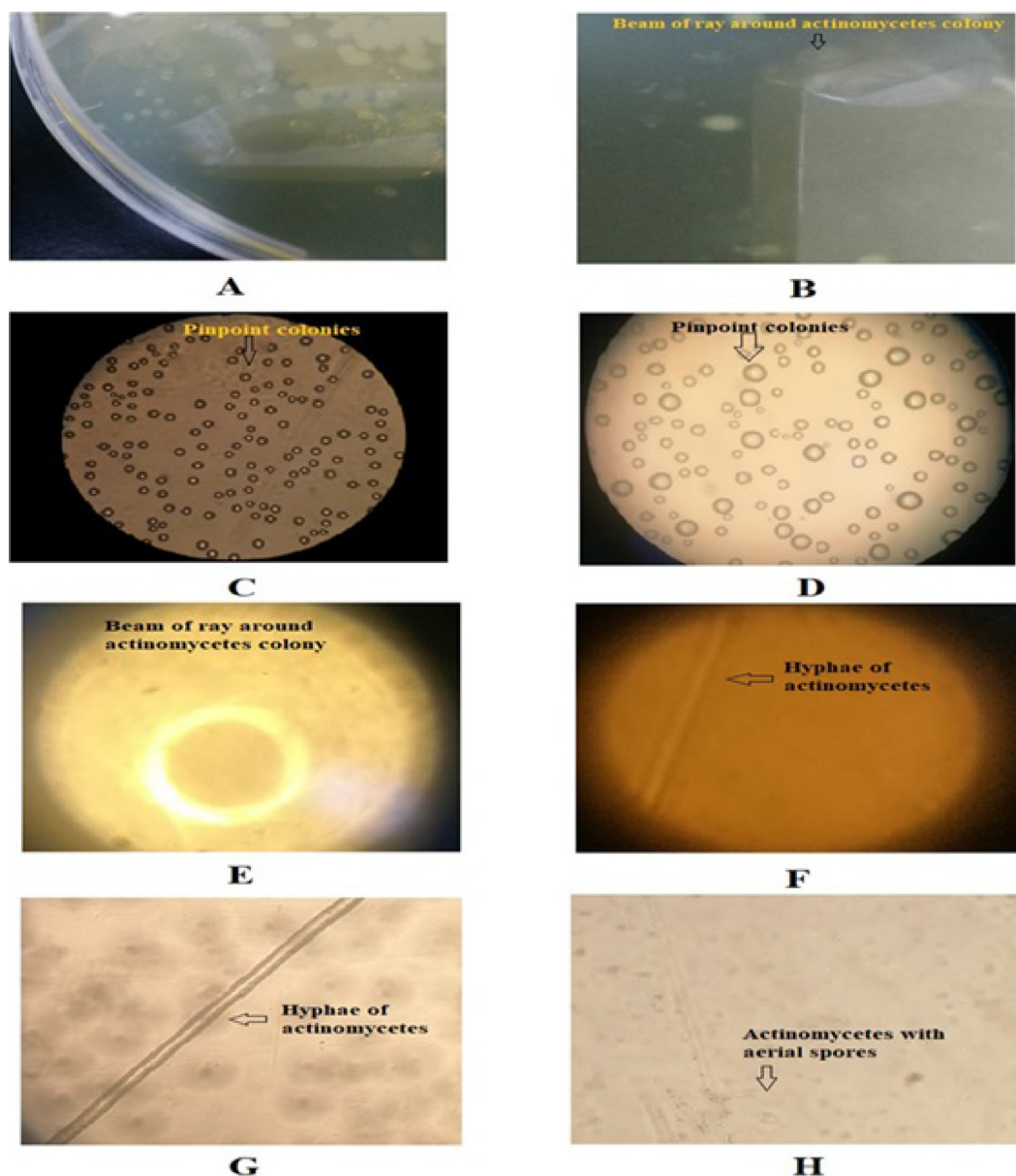
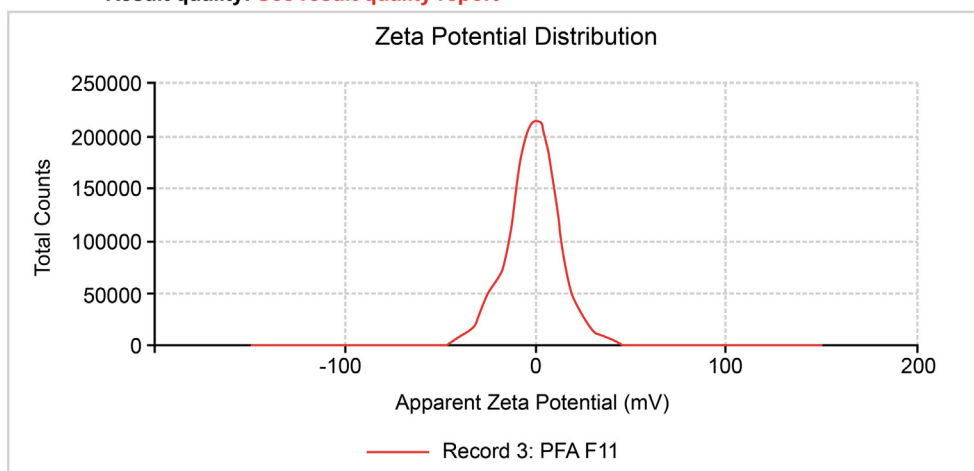


**Fig. 2** Growth pattern and morphological characters of Actinomycetes. (A) Growth of actinomycetes as pinpoint colonies on the agar surface; (B) A sunbeam of ray-like structure observed around pinpoint colonies; (C) Pinpoint colonies of actinomycetes on the agar surface mounted under phase contrast microscope at 150 × magnification; (D) Pinpoint colonies of actinomycetes on the agar surface mounted under phase contrast microscope at 300 × magnification; (E) A sunbeam of ray-like structure observed around pinpoint colonies focused under phase contrast microscope at 600 × magnification; (F) Hyphae of mycelium of actinomycetes mounted on the slide under phase contrast microscope at 150 × magnification; (G) Hyphae of mycelium of actinomycetes mounted on the slide under phase contrast microscope at 600 × magnification; (H) Hyphae of mycelium of actinomycetes under phase contrast microscope at 300 × magnification on the agar surface, showing aerial spores.

## Results

	Mean (mV)	Area (%)	St Dev (mV)
<b>Zeta Potential (mV): -1.42</b>	<b>Peak 1:</b> -1.42	100.0	13.9
<b>Zeta Deviation (mV): 13.9</b>	<b>Peak 2:</b> 0.00	0.0	0.00
<b>Conductivity (mS/cm): 1.28</b>	<b>Peak 3:</b> 0.00	0.0	0.00

Result quality: **See result quality report**

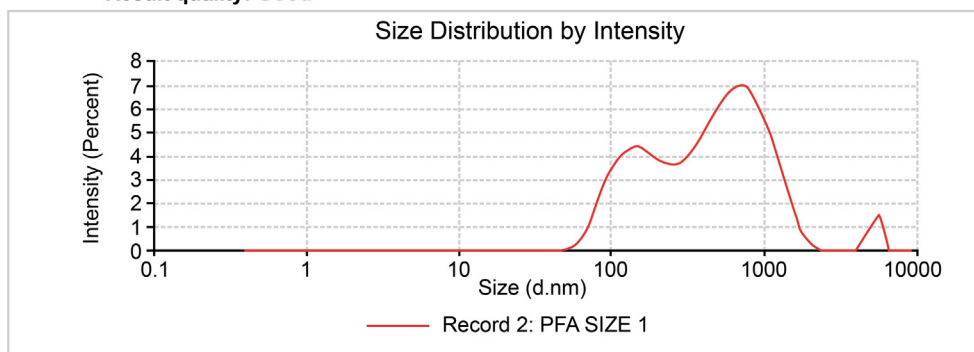


**A**

## Results

	Size (d.nm)	Intensity (%)	St Dev (d.nm)
<b>Z-average (d.nm): 311.2</b>	<b>Peak 1:</b> 692.5	64.4	339.7
<b>Pdi: 0.536</b>	<b>Peak 2:</b> 153.7	33.2	55.45
<b>Intercept: 0.882</b>	<b>Peak 3:</b> 5216	2.5	466.1

Result quality: **Good**



**B**

**Fig. 3 Zeta potential report of the fermented product (FP). (A)** The peak shows the surface charge of the colloidal system in FP **(B)** The peak shows the size distribution analysis and polydispersity index (pdi) of the colloidal system in FP.

from actinomycetes sp. through laboratory-scale fermentation as a prime step for large-scale industrial fermentation processes.

### 3.1. Growth and identification

In this study, actinomycetes sp. was cultivated on SD agar media. The actinomycetes grew as pinpoint colonies on the agar surface. The colonies exhibited a starburst appearance, which is a characteristic feature of actinomycetes (Fig. 2A and 2B). The pinpoint colonies were further observed by

mounting under a phase-contrast microscope at 150 and 300 $\times$  magnifications. Fig. 2C and 2D depict the pinpoint colonies at 150 and 300 $\times$  magnification, respectively. These results confirm the ray-like structure around the pinpoint colonies. Interestingly, further enhancement of the magnification to 600 $\times$  revealed the sunbeam appearance very clearly. The actinomycetes colonies exhibited hyphae (Fig. 2F and 2G). Fig. 2H depicts the colony characteristics with aerial spores. These are the prominent growth characteristics of actinomycetes. Furthermore, Gram staining showed that the bacteria were Gram-positive, and all the biochemical tests were show-

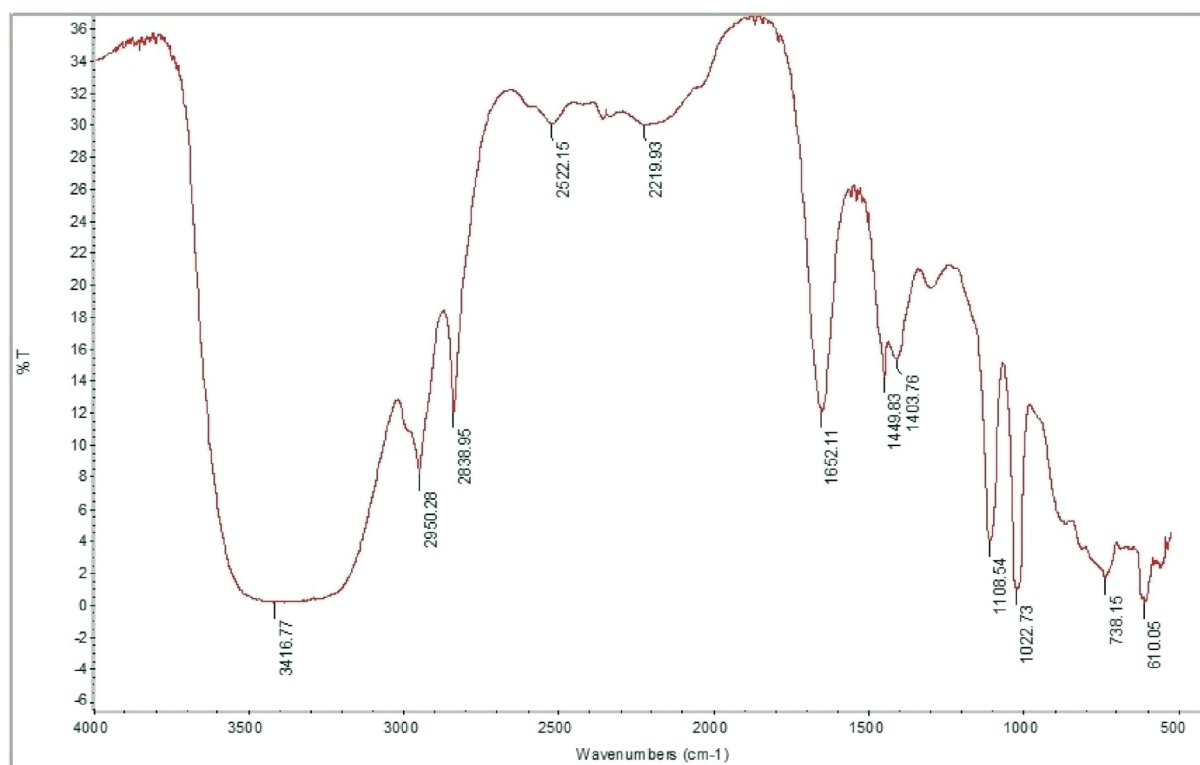


**Fig. 4** FT-IR spectrum of fermented product (FP) scanned at 400–4000  $\text{cm}^{-1}$ .

**Table 1** GC-MS detection of possible bioactive compounds of fermented product (FP).

Compound number	Compound name	Molecular formula	Molecular weight	Retention time (Min)
1	1,8,15,22-tetraaza-2,7,16,21-cyclooctacosane tetrone	$\text{C}_{24}\text{H}_{44}\text{N}_4\text{O}_4$	452	67.29
2	Cyclononasiloxane octadecamethyl	$\text{C}_{18}\text{H}_{54}\text{O}_9\text{Si}_9$	666	63.01
3	Lycoxanthin	$\text{C}_{40}\text{H}_{56}\text{O}$	552	61.07
4	Perylo[1,12-def]-1,3-dioxepin-5,11-dione,6,12-dihydroxy-8,9-bis(2-hydroxypropyl)-7,10-dimethoxy-	$\text{C}_{29}\text{H}_{26}\text{O}_{10}$	534	61.07
5	Ethyl <i>iso</i> -allochololate	$\text{C}_{26}\text{H}_{44}\text{O}_5$	436	60.55
6	Octadecane, 3-ethyl-5-(2-ethylbutyl)	$\text{C}_{26}\text{H}_{54}$	366	55.54
7	Dasycarpidan-1-methanol acetate(ester)	$\text{C}_{20}\text{H}_{26}\text{N}_2\text{O}_2$	326	53.12
8	Hexadecanoic acid, 2, 3- dihydroxy propyl ester	$\text{C}_{19}\text{H}_{38}\text{O}_4$	330	46.17
9	Propanoic acid, 2-(3-acetoxy-4,4,14-trimethylandro-8-en-17-yl)-	$\text{C}_{27}\text{H}_{42}\text{O}_4$	430	43.88
10	Heptadecane, 9-hexyl-	$\text{C}_{23}\text{H}_{48}$	324	43.88
11	Heptacosane	$\text{C}_{27}\text{H}_{56}$	380	37.09
12	Phthalic acid, butyl undecyl ester	$\text{C}_{23}\text{H}_{36}\text{O}_4$	376	32.29

ing positive results which confirmed that the isolates were actinomycetes. Similar kind of studies were reported earlier (Chaudhary et al., 2013b; Dhananjeyan et al., 2010).

### 3.2. Characterization of FP

#### 3.2.1. Zetapotential analysis

The zeta potential is frequently used to characterize the colloidal stability of particles and macromolecules suspended in liquid (Ramaye et al., 2021). An early study suggested that the zeta potential varies depending on whether the fermentation is aerobic or anaerobic in nature (Lucía et al., 2019). The zeta potential results confirmed that the fermentation medium was stable, with a uniform molecular distribution

devoid of sediments, which is an important requirement in the formulation of injectable pharmaceuticals. The zeta potential analysis of the FP presented in Fig. 3 (A) showed a unique pattern of a single peak at  $-0.900$  mV. Zeta size analysis also showed a unique pattern of a single peak with a zeta average size of 2032 (d.nm) and PDI of 0.205 (Fig. 3B). The zeta potential analysis also showed that the quality of the FP revealed a unique and promising peak that expressed the quality of the fermentation medium.

#### 3.2.2. FT-IR analysis

FT-IR spectroscopy of the FP showed the presence of many peaks at various fingerprint regions, which confirmed the presence of functional groups and their respective compounds

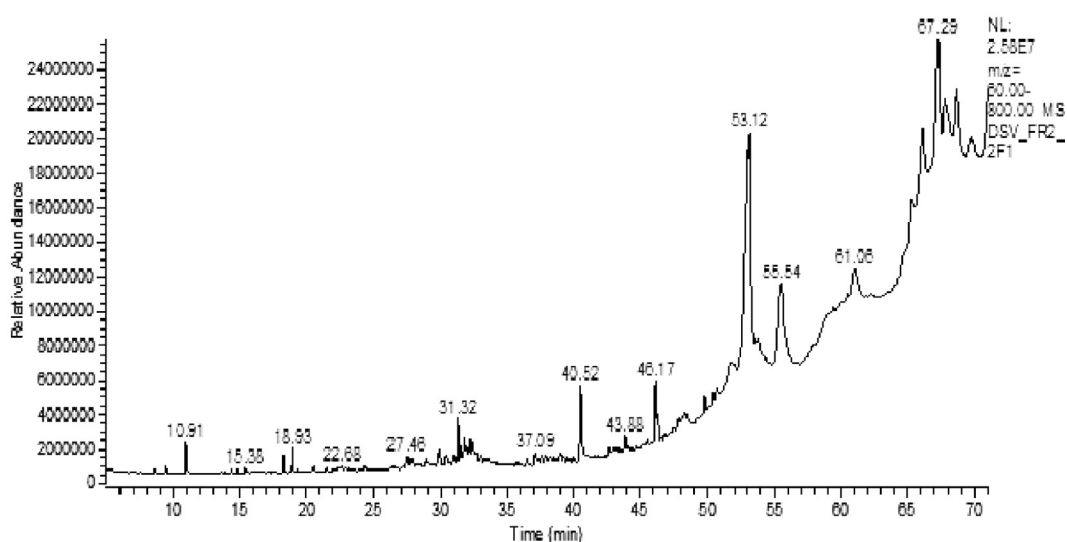


Fig. 5 GC-MS chromatogram of fermented product (FP).

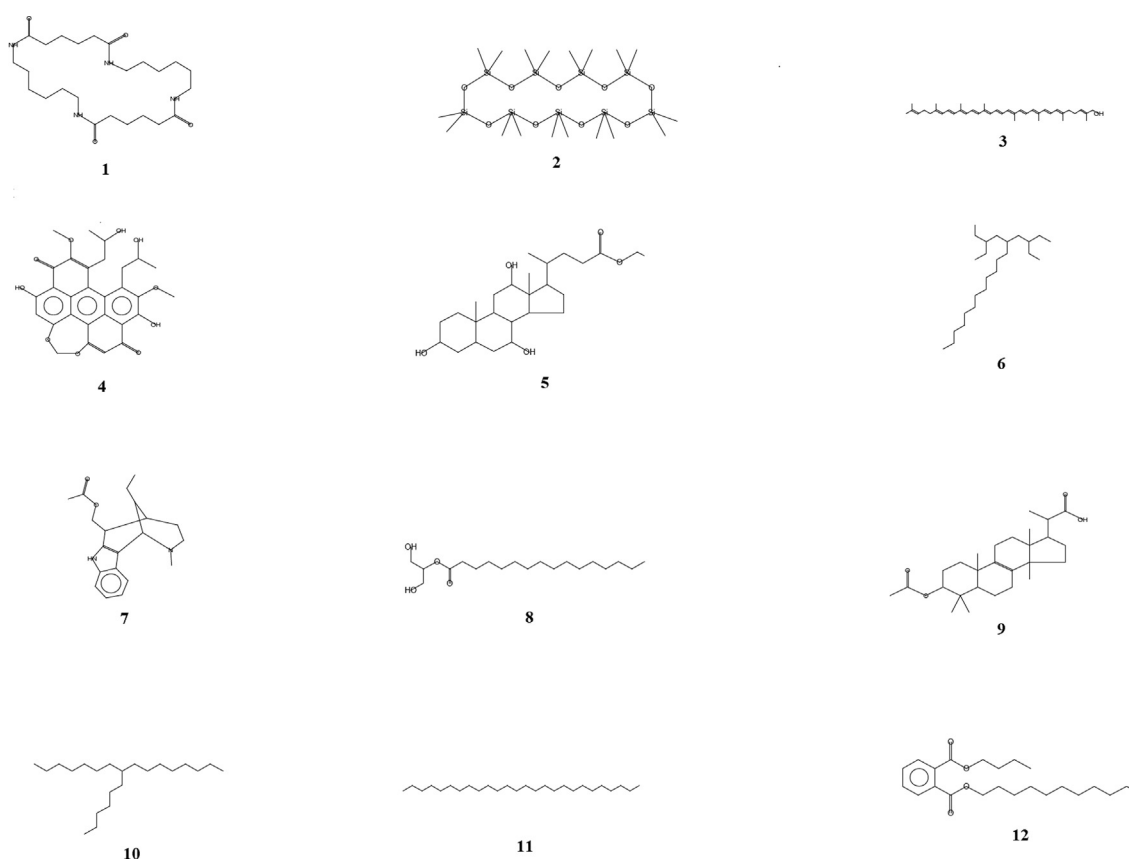


Fig. 6 GC-MS detection of possible bioactive compounds of fermented product (FP). (1) 1,8,15,22-tetraaza-2,7,16,21-cyclooctacosane tetrone (2) Cyclononasiloxane octadecamethyl (3) Lycoxanthin (4) Perylo[1,12-def]-1,3-dioxepin-5,11-dione,6,12-dihydroxy-8,9-bis(2-hydroxypropyl)-7,10-dimethoxy- (5) Ethyl *iso*-allocholate (6) Octadecane, 3-ethyl-5-(2-ethylbutyl) (7) Dasycarpidan-1-methanol acetate (ester) (8) Hexadecanoic acid, 2, 3- dihydroxy propyl ester (9) Propanoic acid, 2-(3-acetoxy-4,4,14-trimethylandro-8-en-17-yl)- (10) Heptadecane, 9-hexyl- (11) Heptacosane (12) Phthalic acid, butyl undecyl ester.

(Fig. 4). The FT-IR spectra were used to identify specific groups that were reflected in GC-MS analysis. Strong sharp peaks appeared at 3416.77, 2950.28, 2838.95, 1652.11,

1108.54, and 1022.73  $\text{cm}^{-1}$ , while weaker peaks were seen at 2522.15, 2219.93, 1449.83, 1403, 738.15 and 610.05  $\text{cm}^{-1}$ . The peak at 3416.77  $\text{cm}^{-1}$  indicates the presence of phenolic

OH groups (strong stretching), and strong-intensity peaks at 2950.28 and 2838.95  $\text{cm}^{-1}$  are attributed to the stretching vibrations of C-H groups and indicate the presence of alkane groups in aliphatic compounds. The strong peaks at 1652.11, 1108.54, and 1022.73  $\text{cm}^{-1}$  represent carboxylic groups (strong stretching), aliphatic ester C-O bonds (strong stretching), and primary alcohols (strong stretching), respectively. Weak peaks at 2522.15 and 2219.93  $\text{cm}^{-1}$  indicate the presence of isothiocyanate groups (strong stretching) and stretching vibrations of alkyne groups with strong intensity, respectively. The medium-intensity peak at 1449.83  $\text{cm}^{-1}$  is attributed to bending vibrations of methyl groups. The peaks at 1403, 738.15 and 610.05  $\text{cm}^{-1}$  are assigned to sulfonyl chloride (strong stretching), alkene (strong bending) and halo (strong stretching) groups, respectively.

### 3.2.3. GC-MS analysis

Table 1 depicting the GC-MS detected bioactive compounds, their molecular formula, molecular weight, and retention time. Unique compounds were identified in the FP through GC-MS analysis. Fig. 5 shows the chromatographic pattern of various compounds in GC-MS analysis, revealing the presence of possible bioactive compounds. The possible structures of the bioactive compounds are displayed in Fig. 6. Table 1 depicting the GC-MS detected bioactive compounds, their molecular formula, molecular weight, and retention time. The study revealed the existence of an indole alkaloid 1,8,15,22-tetraaza-2,7,16,21-cyclooctacosane tetrone, which eluted at a retention time of 67.29 min. However, its specific activity has not yet been established. Cyclononasiloxane octadecamethyl was identified, with a maximum RT of 63 min. An earlier report suggested that cyclononasiloxane octadecamethyl has good antifungal properties (Ni Luh, 2016). In 2017, Taswar et al. (2017) reported the presence of a cyclononasiloxane octade-

camethyl compound produced by *Streptomyces* strain KX852460 in laboratory-scale fermentation. Lycoxanthin, a fungal carotenoid (Echavarri and Johnson, 2002), was observed predominantly in the fermented product of actinomycetes, with a retention time of 61.06 min. Perylo[1,12-def]-1,3-dioxepin-5,11-dione,6,12-dihydroxy-8,9-bis(2-hydroxypropyl)-7,10-dimethoxy- stereoisomer, also called cercosporin, eluted at a retention time of 61.07 min.

Cercosporin, a perylene quinone derivative, is a fungal toxin that damages the host cell by absorbing light energy and producing lipid peroxidation products and reactive oxygen species (ROS) that are toxic to the cell membrane. In this study, the fermentation medium showed a spectrum of antibacterial effects, probably due to the presence of cercosporin. It has been reported that cercosporin also exhibits antiviral potential (Mallika et al., 2012). They demonstrated that the phytoextract of *Septoria pistaciarum* contained cercosporin as one of the compounds with antiprotozoal and antimicrobial effects.

Ethyl *iso*-allocholate, a steroidal compound, eluted at a retention time of 60.55 min. A similar compound exhibiting antimicrobial activity has been reported in the fermentation of *Streptomyces parvulus* (Baskaran et al., 2016). Ethyl *iso*-allocholate has been reported as a component of *Saccharomyces cerevisiae* (Al-Jassani et al., 2016). Propanoic acid, 2-(3-acetoxy-4,4,14-trimethylandro-8-en-17-yl)- was a significant component of the FP. It has been suggested that propanoic acid, 2-(3-acetoxy-4,4,14-trimethylandro-8-en-17-yl)- exhibits antimicrobial and antitumour effects (Azhar et al., 2016). Octadecane, 3-ethyl-5-(2-ethylbutyl), an alkane derivative, was also present, and it has been reported to exert antimicrobial activity (Nguyen et al., 2018). Dasycarpidan-1-methanol (acetate), an alkaloid, is one of the major compounds present in the FP. An earlier study reported that

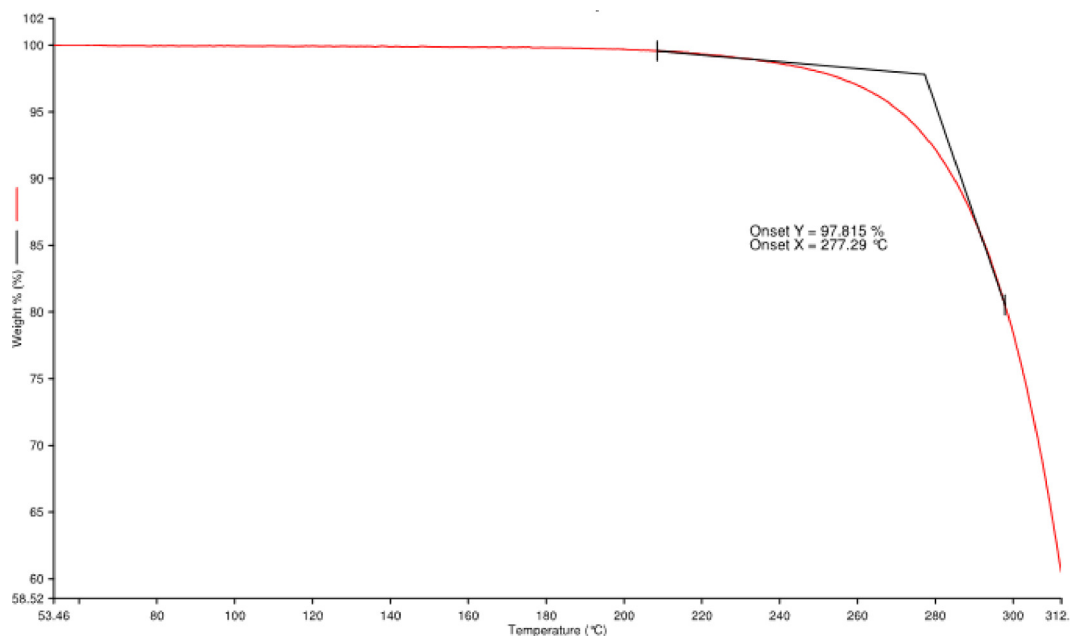
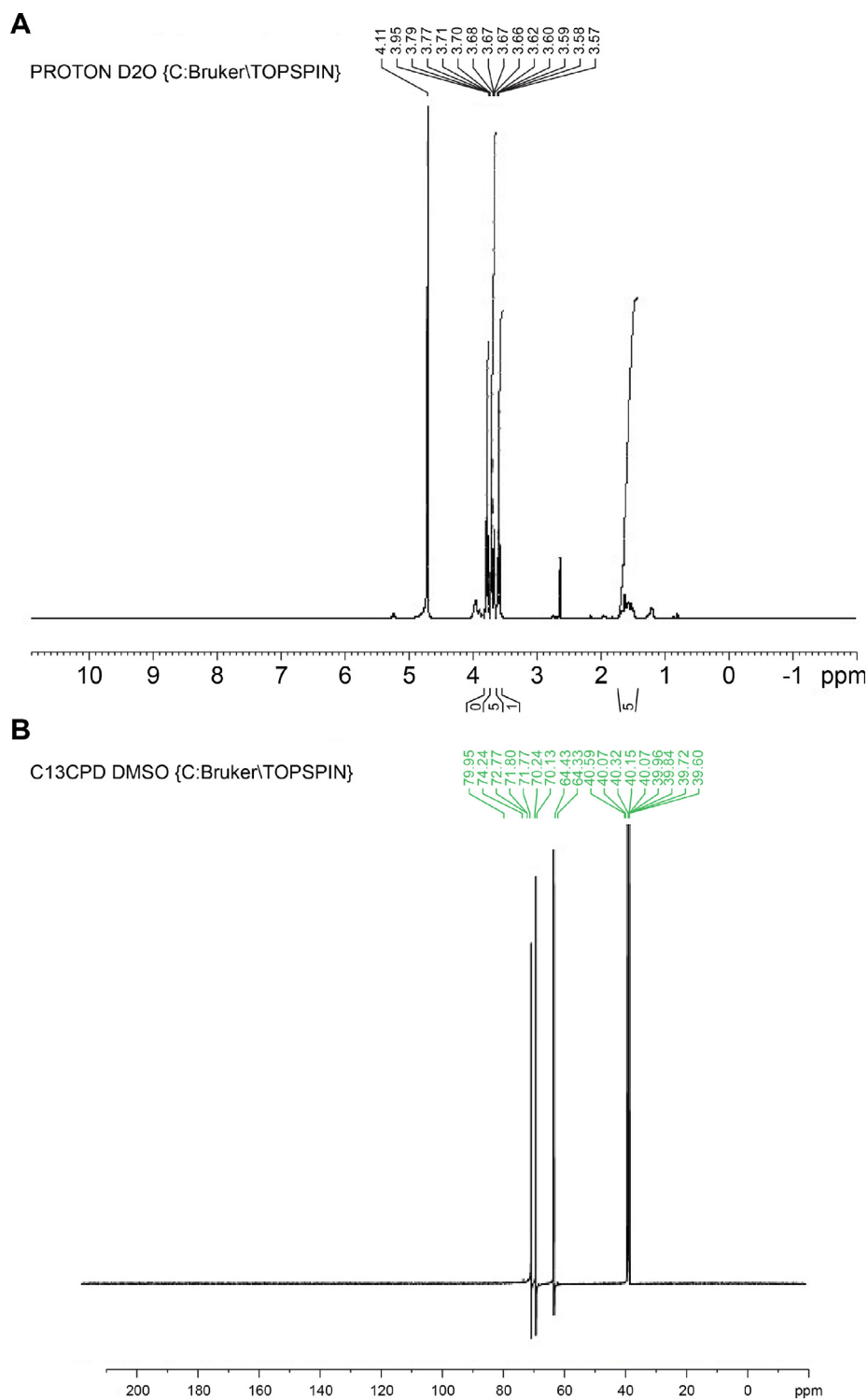


Fig. 7 Thermogravimetric analysis of fermented product (FP).



**Fig. 8** Nuclear Magnetic Resonance study of fermented product (FP). (A)  $^1\text{H}$  NMR fingerprint region (B)  $^{13}\text{C}$  NMR fingerprint region.

dasycarpidan-1-methanol has antimicrobial effect (Sundar and Pillai, 2016; Abeer Fauzi et al., 2017; Abdallah et al., 2019).

Heptadecane, 9-hexyl- was also one of the chief compounds present, and its antifungal properties have been reported (Maghdu and Palaniyappan, 2015). Phthalic acid-butyl was also identified in this study. Recently, phthalic acid-butyl undecyl ester was reported as a metabolic product of the fun-

gus *Penicillium expansum* (Hamza et al., 2015). Octadecane, 3-ethyl-5-(2-ethylbutyl) was observed at 50.66 min in the FP. The compound was eluted in the hexane-acetone extract of the *Penicillium citrinum* ND7a strain, which was reported to have antimicrobial and antifungal activities (Nguyen et al., 2018). Furthermore, the compound was identified in *Streptomyces parvulus* in 2016 (Baskaran et al., 2016). The assessment of

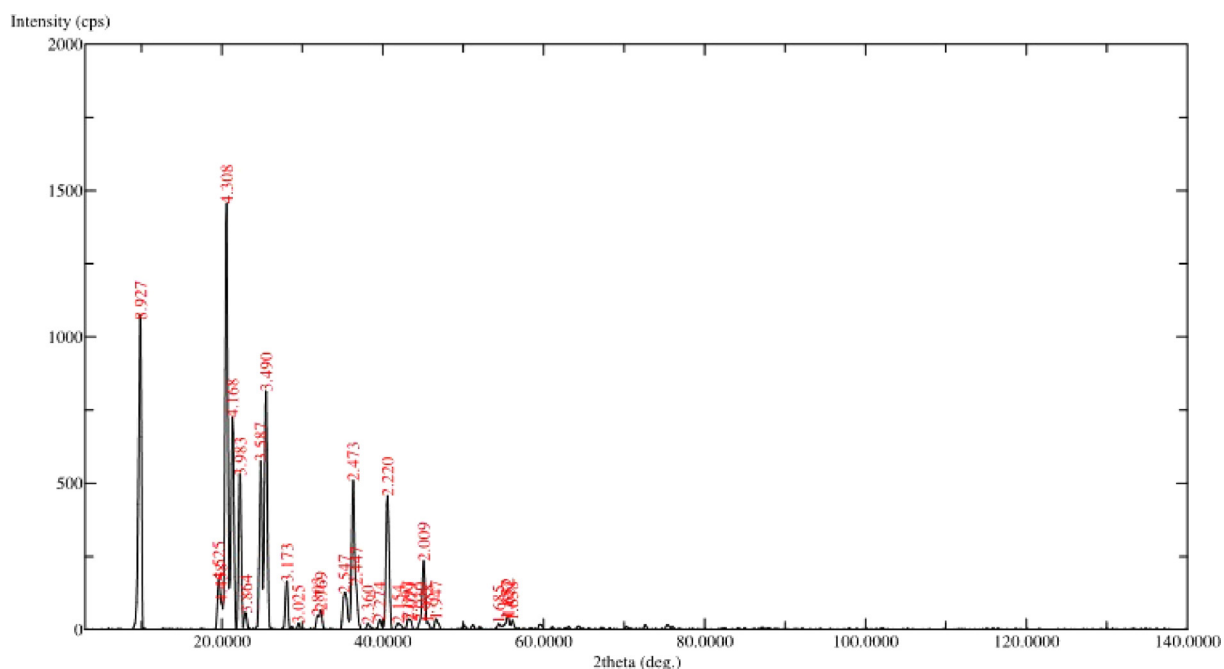


**Fig. 9** XRD analysis of fermented product (FP).

**Table 2** Antibacterial effect of fermented product (FP).

Organisms	Concentration of 24 h culture CFU /mL	Zone of Inhibition (mm)	
		Fermented product (FP)	Ciprofloxacin 5 µg/disc
<i>Bacillus subtilis</i>	$2 \times 10^{-4}$	$20.6 \pm 1.5$ <sup>ns</sup>	$23 \pm 1$
<i>Staphylococcus aureus</i>	$2 \times 10^{-5}$	$18.3 \pm 1.2$ *	$23.3 \pm 0.6$
<i>Streptococcus pyogenes</i>	$2 \times 10^{-4}$	$19.3 \pm 1.5$ *	$24.3 \pm 0.5$
<i>Escherichia coli</i>	$2 \times 10^{-6}$	$21.6 \pm 0.5$ **	$27.3 \pm 0.6$
<i>Pseudomonas aeruginosa</i>	$2 \times 10^{-3}$	$16.3 \pm 1.5$ ***	$25.3 \pm 0.6$
<i>Klebsiella pneumoniae</i>	$2 \times 10^{-3}$	$8.6 \pm 0.6$ ***	$28.7 \pm 2$

# Each value is the mean of 6 batches with standard deviation, ns- nonsignificant, \* P < 0.05 significant; \*\* P < 0.001 highly significant, \*\*\*P < 0.0001 extremely significant. All the values are compared to standard ciprofloxacin disc by performing Tukey Kramer test (post hoc test).

the antibacterial potential of the final product from the FP revealed a good spectrum of activity against the screened human pathogenic bacteria.

#### 3.2.4. TGA

The thermal stability of the FP in the presence of oxygen was measured using Thermogravimetric analysis (TGA). Interestingly, from the thermogram, it can be understood that the initial weight loss in FP was observed at 277.29 °C (Fig. 7). An earlier study demonstrated that Poly-β-hydroxybutyrate (PHB) is a biodegradable polymer, by a rare actinomycete species, *Rhodococcus pyridinivorans* BSRT1-1 showed thermal degradation at 288 °C (Trakunjae et al., 2021). The TGA analysis of polyhydroxybutyrate by *Streptomyces* sp thermo-gravimetric curve ranged from 30 to 860 °C and showed the degradation property at 200 °C about 12.97% and at 400 °C about at 29.47 %. However, complete degradation was observed at 860 °C. Interestingly, FP was started degrading

from 277 °C about 97.815% weight loss was observed, indicating that FP was thermostable.

#### 3.2.5. NMR analysis

The <sup>1</sup>H NMR analysis gave the fingerprint region of FP from 1 to 5 in the proto dimension. The most deshielded proton peak at 3.57, 3.58, 3.59, 3.60, 3.62, 3.65, 3.67, 3.68, 3.70, 3.71, 3.77, 3.79, 3.95 and 4.71 ppm (Fig. 8A). The deshielded peak at 3.57 ppm indicating the presence of methoxy group (Bharti and Roy, 2012). The peak at 3.8 ppm represents the alkoxy proton while the peaks at 3.5–3.6 suggest the presence of aromatic amines (Sivakumar et al., 2021). The <sup>1</sup>H NMR shift from 3.57 to 4.71 ppm indicating the presence of the protons of the glycerol moiety (Alexandri et al., 2017). The prominent peak at 4.71 ppm corresponds to alkene proton. <sup>13</sup>C NMR has been shown to be a very effective approach for determining the distribution of biomolecules. The <sup>13</sup>C NMR spectra of FP is depicting various unique peaks between 39.60 and 79.25 ppm

(Fig. 8B). The peaks correspond to fatty acids, C-N group, methylene group, alkanes, alkyl chloride, alkyl bromide, alkyne, alcohols, and ethers (Wollenberg, 1990; Sivakumar et al., 2021).

### 3.2.6. XRD analysis

The XRD studies are used to characterize the discrete structures. In the current study, XRD analysis at  $2\theta$  revealed distinct particles based on specific diffraction peaks (Fig. 9). The peaks at  $8.927^\circ$ ,  $4.308^\circ$ ,  $4.168^\circ$ ,  $3.983^\circ$ ,  $3.587^\circ$ ,  $3.49^\circ$ ,  $2.473^\circ$  and  $2.220^\circ$  represents  $2\theta$  revealed diffraction peaks (d-values) value of discrete practices in FP. The corresponding  $2\theta$  value for d-values were 9.900, 20.600, 21.300, 22.300, 24.800, 25.500, 36.600 and 40.600 respectively, while the relative intensity (I/I<sub>0</sub>) values of the corresponding d-values were 73, 100, 50, 37, 40, 56, 36 and 32 respectively. Earlier investigations appealed that the XRD patterns of synthesized polymers indicated their polycrystalline character (Nozha et al., 2021; El-Sonbati et al., 2021, 2020; Morgan et al., 2018). As a result, the discrete FP particles may be crystalline in nature. An earlier study suggesting that XRD study was used significantly to detect the polyprenylated benzophenones 7-epi-clusianone (1) and guttiferone A (2) in the organic solvent

extraction of fruits and seed of *Garcinia brasiliensis* (Felipe et al., 2011).

### 3.2.7. Anti-bacterial activity

Table 2 shows the spectrum of antibacterial activity. The readings demonstrate that the antibacterial effect of FP was highest against *Escherichia coli*, followed by *Bacillus subtilis*. The order of antimicrobial effect was *E. coli* > *B. subtilis* > *S. pyogenes* > *S. aureus* > *P. aeruginosa* > *K. pneumoniae*. Except for *K. pneumoniae*, the FP displayed a broad spectrum of antibacterial activity against the pathogens examined. As previously documented, the antibacterial activity of FP may be a result of ligand synthesis on the bacterial membrane (Abou-Dobara et al., 2019; Abou-Dobara et al., 2013). Fig. 10 shows the statistically significant differences between the groups. The efficacy of FP among Gram-positive among Gram-negative bacteria was compared to the control ciprofloxacin in this investigation (Alam et al., 2016). The effectiveness of FP was nonsignificant at  $p < 0.05$  level compared with standard ciprofloxacin against Gram-positive bacteria. Furthermore, among Gram-negative bacteria the efficacy of FP was extremely significant at  $p < 0.05$  level. As a result, the current study concludes that the effectiveness of FP against Gram-positive

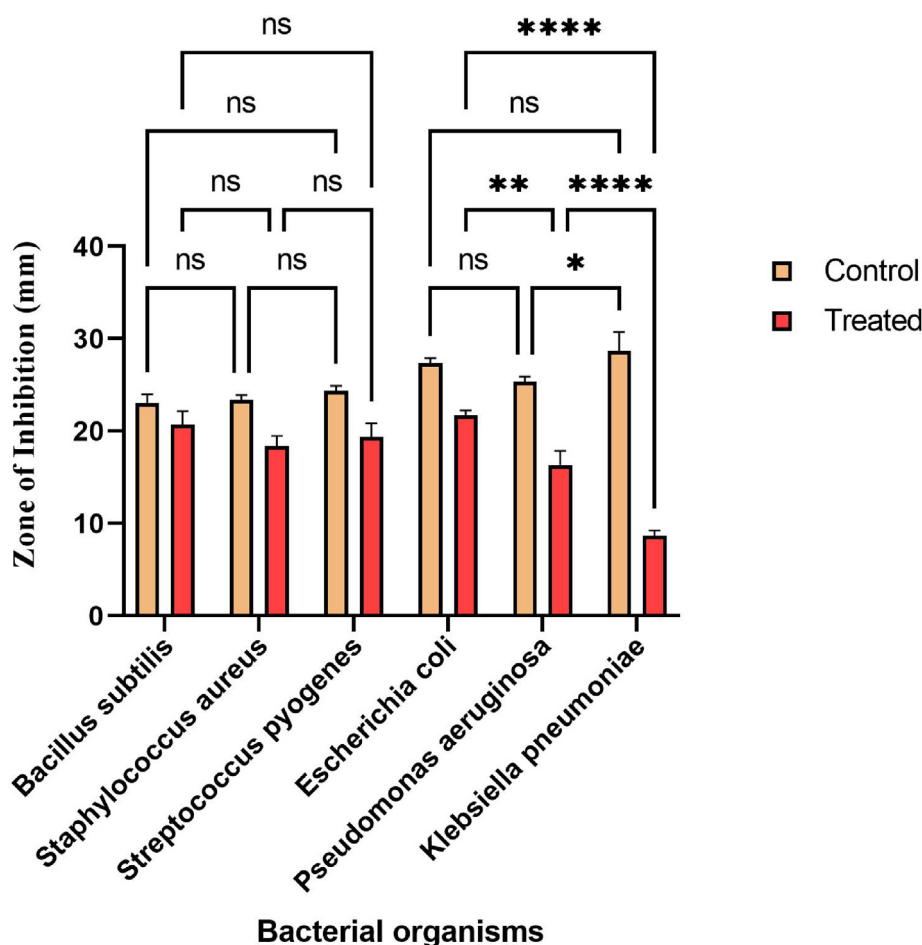


**Fig. 10** The efficacy of fermented product (FP) *Vs* Ciprofloxacin. The statistical significance level was done by performing Tukey Kramer multiple test. \* Significant among compared groups at  $p < 0.05$  level; \*\* High significant among compared groups at  $p < 0.05$  level; \*\*\*\*Extremely significant among compared groups at  $p < 0.05$  level. # ns: nonsignificant among compared groups at  $p < 0.05$  level; Control: Ciprofloxacin disc; Test treated: Fermented product (FP).

bacteria is equivalent to standard ciprofloxacin. But the efficacy of FP against Gram-negative is significantly lesser at  $p < 0.05$  level than the standard ciprofloxacin. An earlier study suggested that isolates of actinomycetes from the soil samples of Sheopur, India exhibited the highest activity against *B. cereus* and *E. faecalis*, respectively (Chaudhary et al., 2013b). Recently, actinomycetes isolated from coal mine site's soils showed good antibacterial and antifungal activity (Kasarla et al., 2021). Based on our experiment, the FP from actinomycetes sp of Rijal Alma soil has a good source of secondary metabolites, and novel antibiotics can be isolated and developed..

#### 4. Conclusion

The concept of developing novel pharmaceutical agents, especially antibiotics, is very important since most of the currently used antibiotics have become ineffective due to the development of resistance through plasmid mediation in microorganisms. Many promising secondary metabolites can be isolated from Actinomycetes sp., a special group of higher bacteria found in soil. Through GC-MS, FT-IR, TGA, NMR, and XRD analyses, the unique secondary metabolites in FP were identified, and the antibacterial potentiality against screened human pathogenic bacteria was investigated. In addition, the research is being streamlined to isolate a specific compound, which will then be structurally elucidated in order to develop a novel antibiotic molecule.

#### Authors contribution

SSA: The principal investigator conceived the design; SSM: Conceptualization, experimentation, processing of results, writing and editing, MHS, MAB & OAM: Project management; SAL & HAM: Collection of data and financial support; ZUR, MSA & SM: Performed experiments; MEE, DB & MZS: collected the data and analysis of the experimental data.

#### CRedit authorship contribution statement

**Saad S. Alqahtani:** Conceived the design and. **Sivakumar S. Moni:** Conceptualization, Experimentation, Processing of results, Writing, and Editing.

#### Acknowledgement

The authors are acknowledging the Deanship of Scientific Research, Jazan University, Jazan, Kingdom of Saudi Arabia, for funding the project. The reference number is Waed project, W41 034.

#### References

Abdallah, M.E., Ali, H.B., Abdel-Wahab, M.A., 2019. Natural products of *Alternaria* sp., an endophytic fungus isolated from *Salvadora persica* from Saudi Arabia. Saudi J. Biol. Sci. 6 (5), 1068–1077. <https://doi.org/10.1016/j.sjbs.2018.04.010>.

Abeer Fauzi, A.R., Ashwak, F.K., Imad, H.H., 2017. Phytochemical screening of methanolic leaves extract of *Malva Sylvestris*. Int. J. Pharmacognosy Phytochem. Res. 9 (4), 537–552.

Abou-Dobara, M.I., El-Sonbati, A.Z., Morgan, Sh.M., 2013. Influence of substituent effects on spectroscopic properties and antimicrobial activity of 5-(4'-substituted phenylazo)-2-thioxothiazolidinone derivatives. World J. Microbiol. Biotechnol. 29, 119–126. <https://doi.org/10.1007/s11274-012-1164-5>.

Abou-Dobara, M.I., Omar, N.F., Diab, M.A., El-Sonbati, A.Z., Morgan, Sh.M., El-Mogazy, M.A., 2019. Allyl rhodanine azo dye derivatives: Potential antimicrobials target D-alanyl carrier protein ligase and nucleoside diphosphate kinase. J. Cell. Biochem. 120, 1667–1678. <https://doi.org/10.1002/jcb.27473>.

Al-Jassani, M.J., Ghaidaa, J.M., Imad, H.H., 2016. Secondary metabolites analysis of *Saccharomyces cerevisiae* and evaluation of antibacterial activity. Int. J. Pharma. Clin. Res. 8 (5), 304–315.

Alam, M.F., Safhi, M.M., Sivakumar, S.M., Aamena, J., 2016. In vitro antibacterial spectrum of sodium selenite against selected human pathogenic bacterial strains. Scientifica 9176273. <https://doi.org/10.1155/2016/9176273>.

Alexandri, E., Ahmed, R., Siddiqui, H., Choudhary, M.I., Tsiafoulis, C.G., Gerothanassis, I.P., 2017. High resolution NMR spectroscopy as a structural and analytical tool for unsaturated lipids in solution. Molecules (Basel, Switzerland) 22 (10), 1663. <https://doi.org/10.3390/molecules22101663>.

Azhar, A.S., Suhaila, H.B., Imad, H.H., 2016. Analysis of bioactive chemical compounds of Euphorbia lathyris using gas chromatography-mass spectrometry and fourier-transform infrared spectroscopy. J. Pharmacognosy Phytother. 8 (5), 109–126. <https://doi.org/10.5897/JPP2015.0371>.

Barsby, T., Kelly, M.T., Gagné, S.M., Andersen, R.J., 2001. Bogorol A produced in culture by a marine Bacillus sp. reveals a novel template for cationic peptide antibiotics. Org. Lett. 3, 437–440. <https://doi.org/10.1021/ol006942q>.

Baskaran, R., Mohan, P.M., Sivakumar, K., Kumar, A., 2016. Antimicrobial activity and phylogenetic analysis of *Streptomyces parvulus* dosmb-d105 isolated from the mangrove sediments of Andaman Islands. Acta Microbiol. Immunol. Hungarica 63 (1), 27–46. <https://doi.org/10.1556/030.63.2016.1.2>.

Bharti, S.K., Roy, R., 2012. Quantitative <sup>1</sup>H NMR Spectroscopy. Trends Analyt. Chem. 35, 5–26. <https://doi.org/10.1016/j.trac.2012.02.007>.

Byrne, M.K., Miellet, S., McGlenn, A., Janaye, F., Shahla, M., Nina, R., van Oijen, A.M., 2019. The drivers of antibiotic use and misuse: the development and investigation of a theory driven community measure. BMC Public Health 19, 1425. <https://doi.org/10.1186/s12889-019-7796-8>.

Catalano, A., Iacopetta, D., Ceramella, J., Scumaci, D., Giuzio, F., Saturnino, C., Aquaro, S., Rosano, C., Sinicropi, M.S., 2022. Multidrug Resistance (MDR): A Widespread Phenomenon in Pharmacological Therapies. Molecules 27, 616. <https://doi.org/10.3390/molecules27030616>.

Chaudhary, H.S., Yadav, J., Shrivastava, A.R., Singh, S., Singh, A.K., Gopalan, N., 2013a. Antibacterial activity of actinomycetes isolated from different soil samples of Sheopur (A city of central India). J. Adv. Pharm. Technol. Res. 4 (2), 118–123. <https://doi.org/10.4103/2231-4040.111528>.

Chaudhary, H.S., Yadav, J., Shrivastava, A.R., Singh, S., Singh, A.K., Gopalan, N., 2013b. Antibacterial activity of actinomycetes isolated from different soil samples of Sheopur (A city of central India). J. Adv. Pharm. Technol. Res. 4, 118–123. <https://doi.org/10.4103/2231-4040.111528>.

Dhananjayan, V., Selvan, N., Dhanapal, K., 2010. Isolation, characterization, screening and antibiotic sensitivity of actinomycetes from locally (Near MCAS) collected soil samples. J. Biol. Sci. 10, 514–519. <https://doi.org/10.3923/jbs.2010.514.519>.

Chloe, T., 2022. Antibiotic-resistant infections are a 'major global health threat' that's killing millions, scientists say. <https://www.cnbc.com/2022/01/20/antibiotic-resistant-infections-are-killing-millions-scientists-say-in-lancet-study.html>

- Echavarri, E.C., Johnson, E.A., 2002. Fungal carotenoids. *Appl. Mycol. Biotechnol.* 2, 45–85. [https://doi.org/10.1016/S1874-5334\(02\)80006-5](https://doi.org/10.1016/S1874-5334(02)80006-5).
- El-Sonbati, A.Z., Omar, N.F., Abou-Dobara, M.I., Diab, M.A., El-Mogazy, M.A., Morgan, S.M., Hussien, M.A., El-Ghettany, A.A., 2021. Structural, molecular docking computational studies and *in vitro* evidence for antibacterial activity of mixed ligand complexes. *J. Mol. Struct.* 1239, <https://doi.org/10.1016/j.molstruc.2021.130481> 130481.
- El-Sonbati, A.Z., Diab, M.A., Morgan, S.M., Abou-Dobara, M.I., El-Ghettany, A.A., 2020. Synthesis, characterization, theoretical and molecular docking studies of mixed-ligand complexes of Cu(II), Ni(II), Co(II), Mn(II), Cr(III), UO<sub>2</sub>(II) and Cd(II). *J. Mol. Struct.* 1200, <https://doi.org/10.1016/j.molstruc.2019.127065> 127065.
- Felipe, T.M., Marcelo, H., dos Santos, C.P., Coelho, L.C.A., Barbosa, G.C., Dias, M.P., Fracca, P.P., Neves, P.C., Stringheta, A.C., Doriguetto, 2011. A powder X-ray diffraction method for detection of polypropylenated benzophenones in plant extracts associated with HPLC for quantitative analysis. *J. Pharm. Biomed. Anal.* 54, 451–457. <https://doi.org/10.1016/j.jpba.2010.09.010>.
- Gupta, R., Gupta, G.D., 2017. Determination of Plant Constituents in fractions of *Cordia alliodora* Willd. Leaf methanol extract using GC-MS analysis. *Int. J. Pharmacogn. Phytochem.* 9 (9), 1274–1279. <https://doi.org/10.25258/phyto.v9i09.10316>.
- Hamza, L.F., Sabreen, A.K., Imad, H.H., 2015. Determination of metabolites products by *Penicillium expansum* and evaluating antimicrobial activity. *J. Pharmacognosy Phytother.* 7 (9), 194–220. <https://doi.org/10.5897/JPP2015.0360>.
- Hawkey, P.M., Warren, R.E., Livermore, D.M., McNulty, C.A.M., Enoch, D.A., Otter, J.A., Wilson, A.P.R., 2018. Treatment of infections caused by multidrug-resistant Gram-negative bacteria: report of the British society for antimicrobial chemotherapy/healthcare infection society/British infection association joint working party S iii2–iii78. *J. Antimicrob. Chemother.* 73 (3). <https://doi.org/10.1093/jac/dky027>.
- Kasarla, S., Gattu, S., Rasiravathanahalli, K.G., Fuad, A., Suaad, A., Al Gwaiz, H.I., Thampu Raja, K., Gangalla, R., 2021. Antimicrobial and antifungal activity of soil actinomycetes isolated from coal mine sites. *Saudi J. Biol. Sci.* 28 (6), 3553–3558. <https://doi.org/10.1016/j.sjbs.2021.03.029>.
- Lazzarini, A., Cavaletti, L., Toppo, G., Flavia, M., 2000. Rare genera of actinomycetes as potential producers of new antibiotics. *Antonie Van Leeuwenhoek* 78, 399–405. <https://doi.org/10.1023/A:1010287600557>.
- Lucía, M.L., Axel, H., Mónica, A.N., Edgardo, A.D., 2019. Zeta potential changes of *Saccharomyces cerevisiae* during fermentative and respiratory cycles. *Colloids Surf. B.* 174, 63–69. <https://doi.org/10.1016/j.colsurfb.2018.11.001>.
- Magarvey, N.A., Jessica, M.K., Valerie, B., Martin, D., David, H.S., 2004. Isolation and characterization of novel marine-derived actinomycete taxa rich in bioactive metabolites. *Appl. Environ. Microbiol.* 70 (12), 7520–7529. <https://doi.org/10.1128/AEM.70.12.7520-7529.2004>.
- Maghdu, N.A., Palaniyappan, K.D., 2015. *In vitro* antifungal potentials of bioactive compounds heptadecane, 9-hexyl and ethyl isoallocholate isolated from *Lepidagathis cristata* Willd. (Acanthaceae) leaf. *Br. Med. Bull.* 3, 336–343. [https://doi.org/10.1016/S1995-7645\(14\)60230-3](https://doi.org/10.1016/S1995-7645(14)60230-3).
- Mallika, K., Khan, S.I., Jacob, M., Tekwani, B.L., Duke, S.O., Ferreira, D., Nanayakkara, N.P., 2012. Antiprotozoal and antimicrobial compounds from the plant pathogen *Septoria pistaciarum*. *J. Nat. Prod.* 75 (5), 883–889. <https://doi.org/10.1021/np200940b>.
- Madkhali, O.A., Sivakumar, S.M., Sultan, M.H., Haitham, A.B., Mohammed, G., Nabil, A.A., Abdulkarim, M.M., Saeed, A., Saad, S.A., Mohammed, A.B., Alam, M.I., Mohamed, E.E., 2021. Formulation and evaluation of injectable dextran sulfate sodium nanoparticles as a potent antibacterial agent. *Sci. Rep.* 11, 9914. <https://doi.org/10.1038/s41598-021-89330-0>.
- Mary Ann, G., John, M., 1967. Slack. Isolation and characterization of *Actinomyces propionicus*. *J. Bacteriol. Res.* 94 (1), 109–115. <https://doi.org/10.1128/jb.94.1.109-115.1967>.
- Moni, S.S., Alam, M.F., Safhi, M.M., Jabeen, A., Sanobar, S., Siddiqui, R., Mookikkal, R., 2018. Potency of nano-antibacterial formulation from *Sargassum binderi* against selected human pathogenic bacteria. *Braz. J. Pharm. Sci.* 54, (4). <https://doi.org/10.1590/s2175-97902018000417811> e17811.
- Mukesh, S., Pinki, D., Meenakshi, C., 2014. Actinomycetes: Sources, Identification, and their applications. *Int. J. Curr. Microbiol. Appl. Sci.* 3 (2), 801–832.
- Morgan, S.M., Diab, M.A., El-Sonbati, A.Z., 2018. Synthesis, molecular geometry, spectroscopic studies, and thermal properties of Co (II) complexes. *Appl. Organometal. Chem.* 32, <https://doi.org/10.1002/aoc.4305> e4305.
- Miethke, M., Pieroni, M., Weber, T., et al, 2021. Towards the sustainable discovery and development of new antibiotics. *Nat. Rev. Chem.* 5, 726–749. <https://doi.org/10.1038/s41570-021-00313-1>.
- Nguyen, T.B., Phan Van, H.L., Cao, N., 2018. Bioactive compounds from marine fungus *Penicillium citrinum* strain ND7c by gas chromatography-mass spectrometry. *Pharm. Chem. J.* 5 (1), 211–224.
- Ni Luh, S., 2016. Identification of the Substance Bioactive Leaf Extract *Piper caninum* Potential as Botanical Pesticides. *Int. J. Pure App. Biosci.* 4 (4), 26–32.
- Nozha, S.G., Morgan, Sh.M., Abu Ahmed, S.E., El-Mogazy, M.A., Diab, M.A., El-Sonbati, A.Z., Abou-Dobara, M.I., 2021. Polymer complexes. LXXIV. Synthesis, characterization, and antimicrobial activity studies of polymer complexes of some transition metals with bis-bidentate Schiff base. *J. Mol. Struct.* 1227, 129525. <https://doi.org/10.1016/j.molstruc.2020.129525>.
- Parungao, M.M., Maceda, E.B.G., Villano, M.A.F., 2007. Screening of antibiotic-producing actinomycetes from marine, brackish and terrestrial sediment of Samal Island, Philippines. *J. Res. Sci. Comput. Eng.* 4 (3), 29–38. <https://doi.org/10.3860/jrsce.v4i3.631>.
- Ramaye, Y., Dabrio, M., Roebben, G., Kestens, V., 2021. Development and validation of optical methods for zeta potential determination of silica and polystyrene particles in aqueous Suspensions. *Materials* 14 (2), 290. <https://doi.org/10.3390/ma14020290>.
- Rogers Van Katwyk, S., Grimshaw, J.M., Nkangu, M., Nagi, R., Mendelson, M., Taljaard, M., Hoffman, S.J., 2019. Government policy interventions to reduce human antimicrobial use: A systematic review and evidence map. *PLoS Med.* 16, (6). <https://doi.org/10.1371/journal.pmed.1002819> e1002819.
- Safhi, M.M., Sivakumar, S.M., Aamena, J., Foziyah, Z., Farah, I., Bagul, U.S., Seyda, S., Tarique, A., Rahimullah, S., Mohammad, A.H.S., Mohamed, E.E., Barik, B.B., Mohammad, F.A., 2016. Therapeutic potential of chitosan nanoparticles as antibiotic delivery system: Challenges to treat multiple drug resistance. *Asian J. Pharm.* 10 (2), S61–S66. <https://doi.org/10.22377/ajp.v10i2.624>.
- Sivakumar, S.M., Mohammad, F.A., Hafiz, A.M., Hassan, A.A., Muhammad, S., Rahimullah, S., Aamena, J., Syeda, S., Shamsheer, M.d., A., Zia, U.R., Mohamed, E.E., Osama, M., Anzarul, H., Mohammed, A., 2021. Solvent extraction, spectral analysis, and antibacterial activity of the bioactive crystals of *Sargassum aquifolium* (Turner) C. Agardh from Red Sea. *Nat. Prod. Res.* 35 (8), 1379–1383. <https://doi.org/10.1080/14786419.2019.1645659>.
- Selim, M.S.M., Abdelhamid, S.A., Mohamed, S.S., 2021. Secondary metabolites, and biodiversity of actinomycetes. *J. Genet. Eng. Biotechnol.* 19 (2021), 72. <https://doi.org/10.1186/s43141-021-00156-9>.
- Sundar, S., Pillai, J.K., 2016. Phytochemical screening and gas chromatograph-mass spectrometer profiling in the leaves of *Solanum incanum* L. *Asian J. Pharm. Clin. Res.* 3, 179–188. <https://innoveareademics.in/journals/index.php/ajpcr/article/view/5246>.
- Taswar, A., Chen, J., Zhao, X., Irfan, M., Wu, Y., 2017. Extraction and identification of bioactive compounds (eicosane and dibutyl

- phthalate) produced by *Streptomyces* strain KX 852460 for the biological control of *Rhizoctonia solani* AG-3 strain KX852461 to control target spot disease in tobacco leaf. *AMB Expr.* 7 (54), 1–9. <https://doi.org/10.1186/s13568-017-0351-z>.
- Trakunjae, C., Boondaeng, A., Apiwatanapiwat, W., Akihiko, K., Takamitsu, A., Kumar, S., Pilanee, V., 2021. Enhanced polyhydroxybutyrate (PHB) production by newly isolated rare actinomycetes *Rhodococcus* sp. strain BSRT1-1 using response surface methodology. *Sci. Rep.* 11, 1896. <https://doi.org/10.1038/s41598-021-81386-2>.
- Wollenberg, K.F., 1990. Quantitative high resolution  $^{13}\text{C}$  nuclear magnetic resonance of the olefinic and carbonyl carbons of edible vegetable oils. *J. Am. Oil Chem. Soc.* 67, 487–494. <https://doi.org/10.1007/BF02540753>.
- Zowawi, H.M., 2016. Antimicrobial resistance in Saudi Arabia. *Saudi Med. J.* 37 (9), 935–940. <https://doi.org/10.15537/smj.2016.9.16139>.